Title

Oxidative Transformation of Nafion-Related Fluorinated Ether Sulfonates: Comparison with Legacy PFAS Structures and Opportunities of Acidic Persulfate Digestion for PFAS Precursor Analysis.

Journal

Environmental Science and Technology, 58(14)

Authors

Liu, Zekun

Jin, Bosen

Rao, Dandan

et al.

Publication Date

2024-04-09

DOI

10.1021/acs.est.3c06289

Peer reviewed

Environmental Science & Technology

pubs.acs.org/est

Article

Oxidative Transformation of Nafion-Related Fluorinated Ether Sulfonates: Comparison with Legacy PFAS Structures and Opportunities of Acidic Persulfate Digestion for PFAS Precursor Analysis

Zekun Liu, Bosen Jin, Dandan Rao, Michael J. Bentel, Tianchi Liu, Jinyu Gao, Yujie Men, and Jinyong Liu*

Cite This: *Environ. Sci. Technol.* 2024, 58, 6415−6424

Read Online

ABSTRACT: The total oxidizable precursor (TOP) assay has been extensively used for detecting PFAS pollutants that do not have analytical standards. It uses hydroxyl radicals ($HO^{\bullet}$) from the heat activation of persulfate under alkaline pH to convert H-containing precursors to perfluoroalkyl carboxylates (PFCAs) for target analysis. However, the current TOP assay oxidation method does not apply to emerging PFAS because (i) many structures do not contain C−H bonds for $HO^{\bullet}$ attack and (ii) the transformation products are not necessarily PFCAs. In this study, we explored the use of classic acidic persulfate digestion, which generates sulfate radicals ($SO_4^{-\bullet}$), to extend the capability of the TOP assay. We examined the oxidation of Nafion-related ether sulfonates that contain C−H or $-COO^-$, characterized the oxidation products, and quantified the F atom balance. The $SO_4^{-\bullet}$ oxidation greatly expanded the scope of oxidizable precursors. The transformation was initiated by decarboxylation, followed by various spontaneous steps, such as HF elimination and ester hydrolysis. We further compared the oxidation of legacy fluorotelomers using $SO_4^{-\bullet}$ versus $HO^{\bullet}$. The results suggest novel product distribution patterns, depending on the functional group and oxidant dose. The general trends and strategies were also validated by analyzing a mixture of 100000- or 10000-fold diluted aqueous film-forming foam (containing various fluorotelomer surfactants and organics) and a spiked Nafion precursor. Therefore, (1) the combined use of $SO_4^{-\bullet}$ and $HO^{\bullet}$ oxidation, (2) the expanded list of standard chemicals, and (3) further elucidation of $SO_4^{-\bullet}$ oxidation mechanisms will provide more critical information to probe emerging PFAS pollutants.

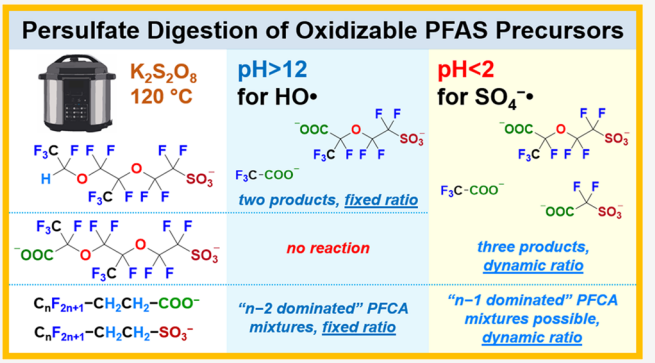

KEYWORDS: *total oxidizable precursor (TOP) assay, Nafion byproducts (NBPs), acid persulfate digestion, fluorotelomer, sulfate radical, hydroxyl radical, aqueous film-forming foam (AFFF), oxidative defluorination*

INTRODUCTION

The study of per- and polyfluoroalkyl substance (PFAS) pollutants has been extended from the early focus on all-carbon perfluoroalkyl carboxylates (PFCAs, $C_nF_{2n+1}-COO^-$) and perfluoroalkanesulfonates (PFSAs, $C_nF_{2n+1}-SO_3^-$) to a large variety of "novel" structures with various heteroatoms, branching patterns, and chain lengths.[1−3] For example, many fluorinated ether structures have been detected in water and soil worldwide[4−7] and shown various toxicities.[8−13] The belated attention to these structures is primarily attributed to (1) the information gap between fluorine chemistry and environmental chemistry and (2) the lack of analytical standards for targeted analysis.[14]

For the detection of telomer ($C_nF_{2n+1}-(CH_2)_m-X$, X = highly diverse organic functional groups) and sulfonamide ($C_nF_{2n+1}-SO_2NH-X$) surfactants, a total oxidizable precursor (TOP) assay has been widely applied.[14] The H atoms in the "precursor" molecules allow oxidation by hydroxyl radicals ($HO^{\bullet}$, generated from persulfate at pH > 12 at 85 °C), yielding one or multiple PFCAs for targeted analysis.[15,16] Our lab further modified the reaction condition (e.g., [NaOH]:[$K_2S_2O_8$] = 5:1 and 120 °C), extended the substrate scope (e.g., $C_nF_{2n+1}-(CH_2)_2-COO^-$, $C_nF_{2n+1}-(CH_2)_2-SO_3^-$, and $HC_nF_{2n}-COO^-$ with variable n) and quantified short-chain products (e.g., CF_3-COO^-, C_2F_5-

Received: August 4, 2023
Revised: March 9, 2024
Accepted: March 11, 2024
Published: March 26, 2024

https://doi.org/10.1021/acs.est.3c06289
Environ. Sci. Technol. 2024, 58, 6415−6424

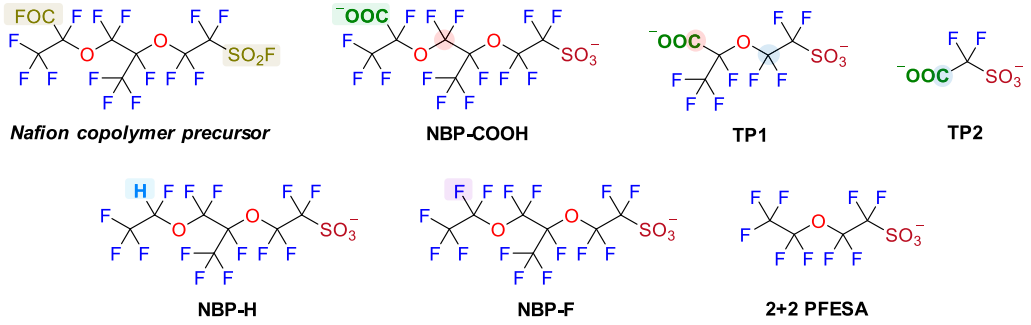

Figure 1. Nafion-related PFAS structures studied in this work.

COO^-, and $^-OOC{-}CF_2{-}COO^-$).[17,18] Notably, structures with only one C−H bond in **H**CF_2− and multiple C−H bonds in −(CH_2)$_2$− showed distinct transformation patterns.[18] A previous TOP assay of various fluoro ether structures by Zhang et al.[19] found that only H-containing structures could be converted by $HO^•$, but the product information remained largely unknown.[20]

The findings presented above reflect several limitations (but not necessarily disadvantages) of the current TOP assay. First, $HO^•$ oxidation requires H atoms in the precursor and does not transform either PFCAs or PFSAs. In contrast, oxidation using sulfate radicals ($SO_4^{-•}$, generated from persulfate and preserved at pH < 2) is a well-adopted pretreatment for water sample analysis. For example, the measurement of total phosphorus uses acidic persulfate digestion to convert various organic phosphate esters into orthophosphate.[21,22] $SO_4^{-•}$ can also oxidize PFCAs via decarboxylation.[23−26] Second, "novel" PFAS structures do not necessarily produce linear PFCAs,[14,19] which the current TOP assay relies on. However, while the reaction kinetics under oxidative conditions have been extensively quantified, the structural transformation of emerging PFAS has not been adequately understood.[20,26] Hence, it is important to elucidate the transformation of novel PFAS "precursors" by both $SO_4^{-•}$ and $HO^•$ for environmental detection and source tracking.

In this work, we examined the oxidative transformation of perfluorinated and polyfluorinated ether sulfonates (PFESAs) related to Nafion polymer production. Nafion membranes are extensively used in the chloralkali electrochemical process[27] and fuel cells.[28] Various "Nafion byproduct" PFESAs have been detected in surface water,[4,5] aquatic animals,[8,29,30] and humans.[31] However, these PFESAs with ether bonds and $-CF_3$ branches (Figure 1) cannot be detected by the current TOP assay.[14] The findings from PFESA oxidation are further compared with those of the extensively studied legacy PFAS to (1) reveal novel mechanistic insights and (2) add new tools for the TOP assay of emerging PFAS pollutants.

MATERIALS AND METHODS

Chemicals. Information on PFAS chemicals, the preparation of stock solutions, and the conversion of structures containing acyl fluoride (−COF) and/or sulfonyl fluoride ($-SO_2F$) into the corresponding carboxylate ($-COO^-$) and/or sulfonate ($-SO_3^-$) are described in the Supporting Information (SI). Potassium persulfate ($K_2S_2O_8$), sulfuric acid (H_2SO_4), and sodium hydroxide (NaOH) were purchased from Fisher Chemical.

Oxidative Reactions. At the elevated temperature, each $S_2O_8^{2-}$ decomposes into two sulfate radicals ($SO_4^{-•}$), which are relatively abundant at pH < 2:

$$S_2O_8^{2-} \rightarrow 2SO_4^{-•}$$

For the oxidation using $SO_4^{-•}$, a 35 mL heavy-walled glass pressure vessel (Synthware Glass, #P160002D) was loaded with 30 mL of the aqueous solution containing 0.5 mM of individual PFAS and variable concentrations of $K_2S_2O_8$ (5−100 mM, 10−200 equiv to PFAS). The initial pH was adjusted by H_2SO_4 to 2.0. The pressure vessels were covered by a threaded cap, which was not closely tightened to avoid pressure buildup. Multiple vessels were vertically immersed in water inside a 250 mL glass beaker. The beaker was placed in a pressure cooker (Farberware 6 Quart, loaded with 1 L of water), which was heated to 120 °C within 20 min and maintained at 120 °C for 40 min. The final pH of the reaction mixture was below 2.0. Without an adequate base, the aqueous solution can be further acidified:

$$SO_4^{-•} + H_2O \rightarrow SO_4^{2-} + HO^• + H^+$$

For the oxidation using $HO^•$, the reaction settings remained the same except that five molar equivalents of NaOH (relative to $K_2S_2O_8$) were also added to ensure pH > 12.0 throughout the reaction. At alkaline pH, $SO_4^{-•}$ radicals are primarily converted to hydroxyl radicals ($HO^•$):

$$SO_4^{-•} + HO^- \rightarrow SO_4^{2-} + HO^•$$

Water Sample Analysis. PFAS parent compounds and transformation products (TPs) were measured by high-performance liquid chromatography equipped with a high-resolution quadrupole Orbitrap mass spectrometer (HPLC−HRMS/MS, Q Exactive, Thermo Fisher Scientific).[17] The instrument settings and quality assurance/control details are provided in the SI. The released fluoride ion (F^-) was measured with an ion-selective electrode (ISE, Fisherbrand Accumet) with a Thermo Scientific Orion Versa Star Pro meter. Each sample was added with an equal volume of total ionic strength adjustment buffer (TISAB for fluoride electrode, Thermo Scientific). The measurement accuracy in the persulfate oxidation matrix has been validated in our previous report.[17] The F^- released from −COF and $-SO_2F$ in the hydrolysis pretreatment was not counted for the oxidative defluorination percentage (deF%).

RESULTS AND DISCUSSION

Oxidation of PFESAs by $HO^•$. We tested six structurally relevant PFESAs (Figure 1). **NBP-COOH** is the hydrolysis product of the *Nafion copolymer precursor*.[5] **NBP-H** (commonly named "*Nafion byproduct 2*") is the decarboxylation product of **NBP-COOH**. **TP1** is a shorter analogue of **NBP-COOH**. **TP2** can be considered as the further shortened "analogue" of **TP1**. **NBP-F** is a fully fluorinated structure without either a $-COO^-$

https://doi.org/10.1021/acs.est.3c06289
Environ. Sci. Technol. 2024, 58, 6415−6424

group or C−H bond on the terminal. **2 + 2 PFESA** can be considered a shorter and linear analogue of **NBP-F**. Instead of meticulously measuring second-order rate constants,[20] we evaluated the reactivity using F^- release as an established rapid probe of oxidative degradation.[17]

As expected, the five structures without a C−H bond for $HO^•$ attack allowed <5% of defluorination (Table 1, entries 2, 6, 11, 22, and 24), whereas **NBP-H** allowed up to 25% of defluorination at $[S_2O_8^{2-}]$:[**NBP-H**] = 100:1 (Table 1, entry 4). The previous study did not identify the oxidation product from **NBP-H**.[20] In this work, following the established "H-abstraction" mechanism by $HO^•$, we predicted that the branched terminal $^•CF(CF_3)-O-R_F$ radical (Scheme 1a) would bind with another $HO^•$ to yield $HO-CF(CF_3)-O-R_F$. This structure with one −F and one −OH on the same carbon would undergo HF elimination to yield the ester $CF_3CO-O-R_F$, which would further hydrolyze under the alkaline condition[32] to afford CF_3COO^- (TFA, inert to $HO^•$ as shown in Table 1, entry 16) and $HO-R_F$. The $HO-R_F$, in this case, would further undergo HF elimination and subsequent hydrolysis to yield **TP1**. With **TP1** as the analytical standard, we verified our prediction and quantified the formation of both **TP1** and TFA (Table 2, zone A). At various $[S_2O_8^{2-}]$:[**NBP-H**] ratios from 10:1 to 100:1, the F atom balance calculated from the residual **NBP-H**, the released F^-, and the **TP1** and TFA products reached 92−99%, indicating the dominance of the simple oxidative pathway under $HO^•$ oxidation. As the $[S_2O_8^{2-}]$:[**NBP-H**] ratio went over 20:1, the formation of **TP1** (0.43−0.47 mM) and TFA (0.42−0.45 mM) were nearly stoichiometric from the initial **NBP-H** (0.5 mM).

Table 1. Oxidative Defluorination of Various PFAS Chemicals

entry	PFAS chemical (**name used in this paper**)	$[S_2O_8^{2-}]$:[PFAS] molar ratio	dominant radical	overall deF (%)[a]
1	$^-OOC-CF(CF_3)-O-CF_2CF(CF_3)-O-CF_2CF_2-SO_3^-$ (**NBP-COOH**)	100:1	$SO_4^{-•}$	46.4
2		100:1	$HO^•$	2.8[b]
3	$H-CF(CF_3)-O-CF_2CF(CF_3)-O-CF_2CF_2-SO_3^-$ (**NBP-H**)	100:1	$SO_4^{-•}$	79.7
4		100:1	$HO^•$	25.0
5	$^-OOC-CF(CF_3)-O-CF_2CF_2-SO_3^-$ (**TP1**)	100:1	$SO_4^{-•}$	76.5
6		100:1	$HO^•$	3.0[b]
7	$^-OOC-CF_2-SO_3^-$ (**TP2**)	10:1	$SO_4^{-•}$	77.9
8		20:1	$SO_4^{-•}$	85.8
9		50:1	$SO_4^{-•}$	88.4
10		100:1	$SO_4^{-•}$	89.5
11		100:1	$HO^•$	1.1[b]
12	CF_3-COO^- (**TFA**)	10:1	$SO_4^{-•}$	53.3
13		20:1	$SO_4^{-•}$	61.8
14		50:1	$SO_4^{-•}$	79.6
15		100:1	$SO_4^{-•}$	90.9
16		100:1	$HO^•$	0.9[b]
17	$C_6F_{13}-CH_2CH_2-SO_3^-$ (**6:2 FTSA**)	100:1	$SO_4^{-•}$	8.3
18		100:1	$HO^•$	54.2
19	$C_6F_{13}-CH_2CH_2-COO^-$ (**6:3 FTCA**)	100:1	$SO_4^{-•}$	41.5
20		100:1	$HO^•$	49.5
21	$CF_3CF_2-O-CF_2CF(CF_3)-O-CF_2CF_2-SO_3^-$ (**NBP-F**)	100:1	$SO_4^{-•}$	4.8[c]
22		100:1	$HO^•$	4.7[c]
23	$CF_3CF_2-O-CF_2CF_2-SO_3^-$ (**2 + 2 PFESA**)	100:1	$SO_4^{-•}$	1.0[c]
24		100:1	$HO^•$	0.4[c]

[a]The calculation considered the total F in the initial PFAS (0.5 mM) to reflect the general efficacy of oxidation. In comparison, the "molecular oxidative deF" in Tables 2 and 3 indicate the average defluorination from each degraded molecule. [b]The limited but significant defluorination at pH > 12 could be attributed to (1) the reaction with a small fraction of $SO_4^{-•}$ radicals before they were quenched by HO^- to yield $HO^•$ or (2) impurities containing C−H or other functional groups that are reactive with $HO^•$. [c]The limited but significant defluorination could be attributed to impurities containing C−H or other functional groups that are reactive with $HO^•$ and $SO_4^{-•}$.

Oxidation of PFESAs by $SO_4^{-•}$. When the oxidant was switched to $SO_4^{-•}$, all structures containing $-COO^-$ allowed significant defluorination (Table 1, entries 1, 3, 5, 10, and 15). As expected, fully fluorinated **NBP-F** and **2 + 2 PFESA** were not reactive (Table 1, entries 21 and 23). Following the established "decarboxylation" mechanism by $SO_4^{-•}$, we predicted that **NBP-COOH** would yield the same $^•CF(CF_3)-O-R_F$ radical (Scheme 1b) as that from the reaction between **NBP-H** and $HO^•$. The carbon radical would bind with another $SO_4^{-•}$ to yield $^-O_3S-O-CF(CF_3)-O-R_F$, which would further hydrolyze under the acidic condition[33] to $HO-CF(CF_3)-O-R_F$. The following steps would yield **TP1** and TFA as described above. However, $SO_4^{-•}$ could further decarboxylate **TP1** following the same set of mechanisms to yield **TP2** and another equivalent of TFA. We verified our prediction and quantified the generation of **TP1**, **TP2**, and TFA from both **NBP-COOH** (Table 2, zone C) and **NBP-H** (Table 2, zone B). The $SO_4^{-•}$ oxidation of **TP1** also generated expected **TP2** and TFA (Table 2, zone D).

A closer data examination led to a series of mechanistic insights. First, when a C−H bond is present in **NBP-H**, the degradation by $SO_4^{-•}$ was much more efficient than by $HO^•$. At the lowest $[S_2O_8^{2-}]$:[**NBP-H**] ratio of 10:1, $SO_4^{-•}$ led to 97.3% degradation of parent **NBP-H**, while $HO^•$ merely resulted in 66.2% degradation. The defluorination from the degraded portion of **NBP-H** by $SO_4^{-•}$ (48.0%) was much higher than that by $HO^•$ (17.7%) because all three transformation products were also reactive with $SO_4^{-•}$.

Second, for the $-COO^-$-containing PFESA structures without a C−H bond, the degradation became more difficult. Within the same time frame, the ratios of $[S_2O_8^{2-}]$:[**NBP-COOH**] and $[S_2O_8^{2-}]$:[**TP1**] needed to be 200:1 to achieve >95% degradation of the parent structures. In particular, the degradation of **NBP-COOH** and **NBP-H** by $SO_4^{-•}$ only differed in the first step (i.e., decarboxylation versus H-abstraction, Scheme 1b), but the defluorination from **NBP-COOH** with all $S_2O_8^{2-}$ doses were lower than from **NBP-H** (Table 2, zone C versus B). **TP1** from **NBP-COOH** or as the starting material (Table 2, zone D) also showed higher recalcitrance than that from **NBP-H**.

https://doi.org/10.1021/acs.est.3c06289
Environ. Sci. Technol. 2024, 58, 6415−6424

Scheme 1. Oxidative Pathways for PFESA Structures by (a) $HO^{\bullet}$ and (b) $SO_4^{-\bullet}$ Radicals

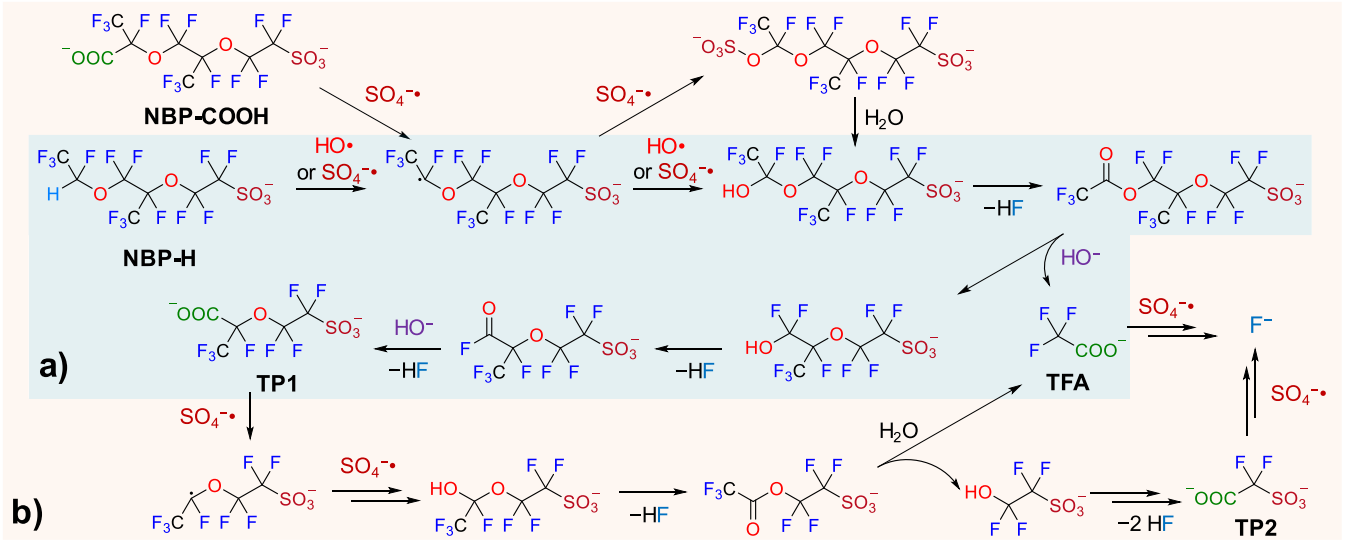

Table 2. Oxidative Transformation of the PFESA Chemicals

$[S_2O_8^{2-}]$:[PFAS] molar ratio	parent PFESA degraded (%)	F^- ion released (mM)	molecular oxidative deF (%)[a]	TP1 (mM)	TP2 (mM)	TFA (mM)	C−F remaining in parent PFESA and targeted TPs (mM)	F atom balance (%)[b]
$H{-}CF(CF_3){-}O{-}CF_2CF(CF_3){-}O{-}CF_2CF_2{-}SO_3^-$ (**NBP-H**) (0.5 mM, containing 7.0 mM C−F)								
A. by $HO^{\bullet}$ (pH > 12)								
10:1	66.2	0.82	17.7	0.31	n.d.	0.32	5.80	95.0
20:1	96.0	1.41	20.9	0.43	n.d.	0.42	4.98	91.9
50:1	98.6	1.61	23.3	0.45	n.d.	0.44	5.02	95.0
100:1	99.4	1.74	25.0	0.47	n.d.	0.45	5.15	99.1
B. by $SO_4^{-\bullet}$ (pH < 2)								
10:1	97.3	3.27	48.0	0.17	0.13	0.30	2.71	84.9
20:1	98.8	3.83	55.3	0.10	0.06	0.26	1.78	79.9
50:1	99.3	4.60	66.2	0.08	0.06	0.16	1.29	84.0
100:1	99.6	5.56	79.7	0.01	0.03	0.08	0.41	85.9
200:1	99.3	6.08	87.5	n.d.	n.d.	0.01	0.08	88.1
$^-OOC{-}CF(CF_3){-}O{-}CF_2CF(CF_3){-}O{-}CF_2CF_2{-}SO_3^-$ (**NBP-COOH**) (0.5 mM, containing 7.0 mM C−F)								
C. by $SO_4^{-\bullet}$ (pH < 2)								
10:1	60.0	1.91[c]	18.9	0.07	0.05	0.06	3.66	65.3
20:1	67.0	2.34[c]	24.9	0.11	0.09	0.04	3.52	69.4
50:1	78.8	3.52[c]	39.9	0.20	0.09	0.07	3.44	85.1
100:1	88.5	4.71[c]	52.4	0.22	0.07	0.06	2.87	94.0
200:1	96.7	5.82[c]	62.3	0.11	0.03	0.10	1.45	89.5
$^-OOC{-}CF(CF_3){-}O{-}CF_2CF_2{-}SO_3^-$ (**TP1**) (0.5 mM, containing 4.0 mM C−F)								
D. by $SO_4^{-\bullet}$ (pH < 2)								
10:1	56.0	4.28[c]	59.8	0.22	0.06	0.16	2.36	100.7
20:1	67.5	4.75[c]	58.2	0.16	0.10	0.12	1.86	95.7
50:1	75.8	5.40[c]	62.7	0.12	0.09	0.12	1.49	96.7
100:1	89.8	6.50[c]	68.2	0.05	0.03	0.09	0.74	94.9
200:1	96.7	6.87[c]	68.1	0.02	0.002	n.d.	0.14	85.8

[a]The calculation considered the degraded portion rather than the total initial PFESA. For **NBP-COOH** and **TP1**, the F^- released from hydrolysis was excluded (see footnote *c*). [b]Including both oxidation-released F^- and all C−F bonds in the remaining parent PFAS and targeted TPs. A significant gap from 100% suggests the formation of unknown TPs. [c]Including F^- released from the hydrolysis of sulfonyl fluoride ($-SO_2F$) and acyl fluoride (−COF) in the precursor chemicals for **NBP-COOH** and **TP1**. The 2 equiv of F^- (1.0 mM) was not considered in the calculation of oxidative defluorination and F atom balance.

Third, following the known mechanisms, oxidative defluorination is realized via a series of "spontaneous" pathways after the oxidants add a −OH to the fluorinated carbon. The pathways include HF elimination from $-C(OH)F-$, hydrolysis of $-C(O)F$, and hydrolysis of ester $CF_3CO{-}O{-}R_F$. Thus, all transformation products are expected to include a $-COO^-$,

https://doi.org/10.1021/acs.est.3c06289
Environ. Sci. Technol. 2024, 58, 6415−6424

Table 3. Oxidative Transformation of C_6F_{13}− Fluorotelomer Carboxylate and Sulfonate

$[S_2O_8^{2-}]$:[PFAS] molar ratio	parent PFAS degraded (%)	F^- ion in the solution (mM) and oxidative deF (%)[a]	C_nF_{2n+1}−COO^- products (mM)						F atom balance (%)[b]
			TFA (n = 1)	PFPrA (n = 2)	PFBA (n = 3)	PFPeA (n = 4)	PFHxA (n = 5)	PFHpA (n = 6)	
C_6F_{13}−CH_2CH_2−SO_3^- (**6:2 FTSA**) (0.5 mM, containing 6.5 mM C−F)									
E. by $SO_4^{-\bullet}$ (pH < 2)									
10:1	31.0	0.19 (9.6)	n.d.	n.d.	n.d.	0.004	0.004	0.004	74.0
20:1	44.5	0.29 (9.9)	n.d.	n.d.	0.004	0.007	0.007	0.004	63.4
50:1	58.8	0.36 (9.5)	n.d.	n.d.	0.004	0.007	0.009	0.005	50.8
100:1	83.3	0.54 (10.0)	n.d.	n.d.	0.007	0.013	0.014	0.007	31.4
F. by $HO^\bullet$ (pH > 12)									
10:1	85.3	2.44 (44.1)	0.025	0.042	0.055	**0.101**	0.079	0.010	92.1
20:1	99.4	3.16 (48.9)	0.045	0.076	0.092	**0.108**	0.042	0.004	90.0
50:1	>99.8	3.50 (53.9)	0.051	0.057	0.064	**0.123**	0.052	0.008	94.9
100:1	>99.8	3.52 (54.2)	0.014	0.042	0.069	**0.128**	0.064	0.019	97.7
C_6F_{13}−CH_2CH_2−COO^- (**6:3 FTCA**) (0.5 mM, containing 6.5 mM C−F)[c]									
G. by $SO_4^{-\bullet}$ (pH < 2)									
10:1	>99.8	1.31 (20.1)	0.015	0.024	0.032	0.062	0.127	0.015	59.2
20:1	>99.8	1.65 (25.3)	0.034	0.036	0.040	0.060	0.069	0.008	55.5
50:1	>99.8	1.91 (29.4)	0.044	0.051	0.051	0.060	0.052	0.007	59.4
100:1	>99.8	2.70 (41.5)	0.048	0.048	0.039	0.037	0.028	0.004	62.4
H. by $HO^\bullet$ (pH > 12)									
10:1	>99.8	3.36 (51.7)	0.049	0.048	0.062	**0.128**	0.051	0.008	92.2
20:1	>99.8	3.32 (51.0)	0.033	0.037	0.071	**0.120**	0.052	0.013	91.0
50:1	>99.8	3.33 (51.3)	0.024	0.035	0.069	**0.115**	0.065	0.018	93.2
100:1	>99.8	3.22 (49.5)	0.021	0.033	0.072	**0.112**	0.066	0.023	92.0

[a]The calculation considered the degraded portion rather than the total initial FTSA/FTCA. [b]Including both oxidation-released F^- and all C−F bonds in the remaining parent PFAS and targeted TPs. A significant gap from 100% suggests the formation of unknown TPs. [c]Further processed data of previously reported experiments (Tables S3 and S5 of ref 17).

Table 4. Oxidative Transformation of *n*:3 Fluorotelomer Carboxylates

C_nF_{2n+1}−CH_2CH_2−COO^- (***n*:3 FTCA**) (0.5 mM, containing [n + 0.5] mM C−F)	parent FTCA degraded (%)	F^- ion in the solution (mM) and oxidative deF (%)[a]	C_nF_{2n+1}−COO^- products (mM)						F atom balance (%)[b]
			TFA (n = 1)	PFPrA (n = 2)	PFBA (n = 3)	PFPeA (n = 4)	PFHxA (n = 5)	PFHpA (n = 6)	
I. by $SO_4^{-\bullet}$ (pH < 2), $[S_2O_8^{2-}]$:[**FTCA**] = 10:1									
n = 1	>99.8	1.17 (78.2)	0.053						88.9
n = 2	>99.8	1.86 (74.3)	**0.091**	0.017					88.6
n = 3	>99.8	2.09 (59.7)	0.089	**0.092**	0.019				84.3
n = 4	>99.8	2.18 (48.5)	0.067	0.082	**0.113**	0.021			83.9
n = 5	>99.8	1.61 (29.2)	0.033	0.045	0.067	**0.072**	0.015		58.4
n = 6[c]	>99.8	1.24 (19.0)	0.019	0.017	0.033	0.054	**0.095**	0.014	51.2
J. by $HO^\bullet$ (pH > 12), $[S_2O_8^{2-}]$:[**FTCA**] = 10:1[d]									
n = 1	>99.8	1.43 (95.0)	n.d.						95.0
n = 2	>99.8	1.90 (76.2)	0.075	0.007					86.5
n = 3	>99.8	2.46 (70.3)	**0.127**	0.081	0.004				93.6
n = 4	>99.8	2.91 (64.6)	0.064	**0.112**	0.036	0.005			88.0
n = 5	>99.8	3.26 (59.2)	0.059	0.079	**0.101**	0.040	0.005		90.1
n = 6[e]	>99.8	3.36 (51.7)	0.049	0.048	0.062	**0.128**	0.051	0.008	92.2

[a]The calculation considered the total initial FTCA because the parent structure degradation had reached >99.8%. [b]Including all C−F bonds in the targeted PFCA TPs because parent FTCA degradation had completed. A significant gap from 100% suggests the formation of unknown TPs. [c]This experiment had the same settings with the first line in Table 3 zone G. [d]Further processed data of previously reported experiments (Figure 2 of ref 17). [e]This experiment had the same settings with the first line in Table 3 zone H.

being subject to further degradation by $SO_4^{-\bullet}$. In theory, 100% oxidative defluorination can be expected, but experimental results found limited defluorination of **NBP-COOH** (62.3%) and **TP1** (68.1%) at a high $S_2O_8^{2-}$ dose of 200:1 (Table 2, zones C and D). Even for the simple molecule **TP2**, the defluorination appeared to be limited at ∼90% (Table 1, entries 7−10). Therefore, other unknown pathways and mechanisms exist for $SO_4^{-\bullet}$ oxidation. This insight is further evidenced by the larger

https://doi.org/10.1021/acs.est.3c06289
Environ. Sci. Technol. 2024, 58, 6415−6424

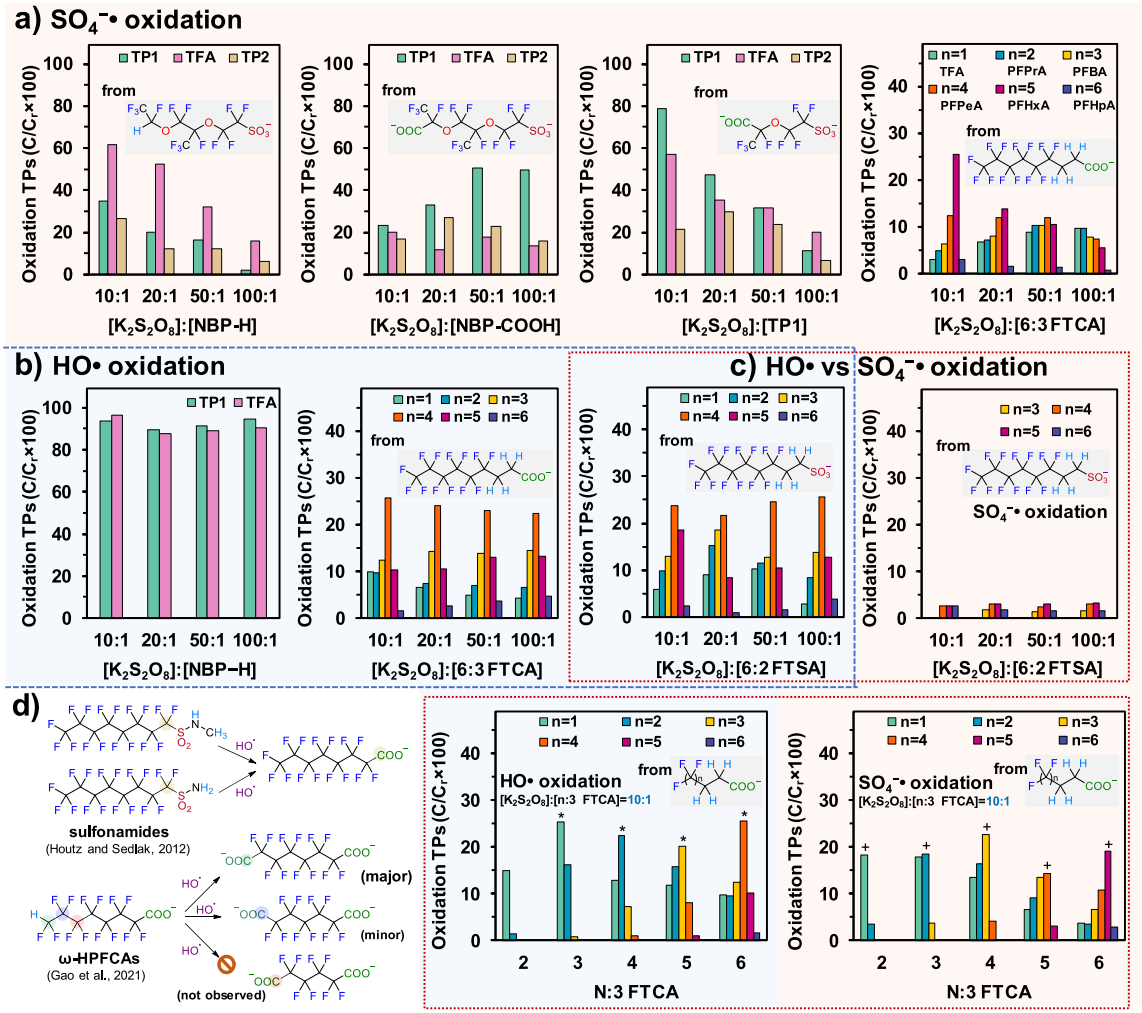

Figure 2. Product distribution by (a) $SO_4^{-\bullet}$ (orange background) and (b) $HO^\bullet$ (blue background) oxidation at varying persulfate doses; (c) comparison of products by $HO^\bullet$ versus $SO_4^{-\bullet}$ from **6:2 FTSA** at varying persulfate doses and from various FTCAs at $[S_2O_8^{2-}]$:[PFAS] = 10:1; (d) two reported characteristic product formation from perfluoroalkane sulfonamides and omega-hydro PFCAs. Note: C_r indicates the degraded portion of the parent PFAS.

gap of F atom balance for $SO_4^{-\bullet}$ than for $HO^\bullet$ (Table 2, zones B and C versus zone A). We did not detect other meaningful TPs via HRMS analyses.

Comparison with the Oxidation of Fluorotelomers. We compared the oxidative transformation patterns of fluorotelomers to those of the "legacy PFAS precursors". For the extensively studied $C_6F_{13}-CH_2CH_2-SO_3^-$ (**6:2 FTSA**), the degradation and defluorination by $SO_4^{-\bullet}$ were much more difficult than by $HO^\bullet$ (Table 3, zone E versus F). When $HO^\bullet$ was used for the heated oxidation, all shorter-chain PFCAs were generated, with the $n-2$ PFCA as the most abundant product (e.g., $C_4F_9-COO^-$ from $C_6F_{13}-CH_2CH_2-SO_3^-$).[15,17] The defluorination, PFCA product distribution, and F atom balance (90−98%) were rather consistent at various $S_2O_8^{2-}$ doses. In contrast, when $SO_4^{-\bullet}$ was used, short-chain PFCAs were negligible, and the defluorination appeared to have an ∼10% limit despite more **6:2 FTSA** being degraded at higher $S_2O_8^{2-}$ doses. An increasingly lower F atom balance (from 74 to 31%) was also observed, suggesting unknown oxidative pathways and mechanisms.

Notably, the carboxylate analogue $C_6F_{13}-CH_2CH_2-COO^-$ (**6:3 FTCA**) showed different behaviors from **6:2 FTSA**. A low oxidant dose at $[S_2O_8^{2-}]$:[**6:3 FTCA**] = 10:1 achieved complete parent structure degradation for both $SO_4^{-\bullet}$ and $HO^\bullet$. We attributed the much higher reactivity of FTCA than FTSA to the weaker C−H bond on the α carbon adjacent to the $-COO^-/-SO_3^-$ group.[17] However, we still cannot explain how this "local" structural difference caused vastly different levels of defluorination by $SO_4^{-\bullet}$ (Table 3, zone G versus E). In the case of **6:3 FTCA**, we observed an obvious shift of the PFCA product dominance from long chain to shorter chain when the $S_2O_8^{2-}$ dose was raised. The rather consistent F atom balance (56−62%) and the increased deF% suggest the defluorination via decarboxylation and the subsequent chain-shortening of PFCA products by $SO_4^{-\bullet}$. Still, other unknown pathways and mechanisms are responsible for the ∼40% gap in the F atom balance. For comparison, $HO^\bullet$ oxidation of FTCA and FTSA showed very similar results in deF%, PFCA product distribution, and high F atom balance (Table 3, zone H versus F).

The extended comparison using various chain lengths of the "most oxidizable" ***n*:3 FTCAs** showed the dominance of $n-2$ PFCA in the products from $HO^\bullet$ oxidation (Table 4, zone J). Elevating the $S_2O_8^{2-}$ doses did not significantly alter the PFCA product distribution (Table 3, zones F and H) because $HO^\bullet$ does not degrade any PFCA. In comparison, $SO_4^{-\bullet}$ oxidation using the low dose of $[S_2O_8^{2-}]$:[***n*:3 FTCA**] = 10:1 yielded the

https://doi.org/10.1021/acs.est.3c06289
Environ. Sci. Technol. 2024, 58, 6415−6424

Table 5. Oxidative Transformation of Diluted AFFF and Spiked NBP-COOH at Sub-μM Levels

		oxidation products (μM)[a]							
$K_2S_2O_8$ (mM)	NaOH (mM)	**NBP-COOH** remained	**TP1**	**TP2**	PFBA (n = 3)	PFPeA (n = 4)	PFHxA (n = 5)	PFHpA (n = 6)	PFOA (n = 7)
K. by $HO^•$ (pH > 12), 100000× diluted AFFF + 0.35 μM **NBP-COOH**, 9.5 mg L^{-1} of organic carbon									
5	25	0.327	0.012	n.d.	0.065	**0.109**	0.050	0.031	0.020
20	100	0.351	0.029	n.d.	0.064	**0.106**	0.035	0.025	0.017
60	300	0.343	n.d.	n.d.	0.113	**0.119**	0.050	0.036	0.016
L. by $SO_4^{-•}$ (pH < 2), 100000× diluted AFFF + 0.35 μM **NBP-COOH**, 9.5 mg L^{-1} of organic carbon									
5		0.115	0.126	0.039	0.055	0.068	**0.095**	0.024	0.017
20		0.031	0.050	0.008	0.025	0.023	0.019	0.008	0.005
60		0.013	0.034	n.d.	0.021	0.013	0.008	0.004	0.002
M. by $SO_4^{-•}$ (pH < 2), 10000× diluted AFFF + 3.5 μM **NBP-COOH**, 95 mg L^{-1} of organic carbon									
5		3.283	1.792	0.533	0.392	0.475	0.568	0.168	0.162
20		0.934	1.354	0.435	0.481	0.476	0.450	0.144	0.126
60		0.242	0.492	0.048	0.494	0.376	0.220	0.093	0.048
N. by $SO_4^{-•}$ (pH < 2), 10000× diluted AFFF, no **NBP-COOH**, 95 mg L^{-1} of organic carbon									
5		n.d.	n.d.	n.d.	0.399	0.458	0.664	0.188	0.188
20		n.d.	n.d.	n.d.	0.459	0.450	0.389	0.154	0.095
60		n.d.	n.d.	n.d.	0.352	0.256	0.166	0.071	0.048

[a]The LC−MS/MS instrument setting did not allow the detection of ultrashort PFCAs, TFA (n = 1) and PFPrA (n = 2).

most dominant product as n − 1 PFCA. Elevating the $S_2O_8^{2-}$ doses shifted the product distribution to short-chain PFCAs (Table 3, zones G). However, due to the limited capability of $SO_4^{-•}$ oxidation, even with a large excess of $S_2O_8^{2-}$ at 100:1, all PFCA products were still detected after oxidative digestion, leaving various evidence for "forensic analysis" of the parent structures.

Implications to PFAS Precursor Analyses. The results presented above suggest a series of similarities and differences between $SO_4^{-•}$ and $HO^•$ for the oxidation of legacy and emerging "PFAS precursors" and their potential value for PFAS sample analyses. First of all, both radicals are destructive to the reactive PFAS structures. The defluorination from **NBP-H**, **6:2 FTSA**, and **6:3 FTCA** by $HO^•$ reached 25, 54, and 52%, respectively (parent compound degradation >99.8%). Because $SO_4^{-•}$ can also oxidize the C−H bond and further degrade PFCAs, the molecular defluorination (i.e., calculated for the degraded portion) of **NBP-H** reached 48−88% with varying $S_2O_8^{2-}$ doses. Therefore, the sum of target PFAS structures after oxidative sample treatment with either $SO_4^{-•}$ or $HO^•$ cannot indicate the total amount of C−F bonds in the original sample. It is also critical to note that different types of PFAS can allow very different levels of defluorination (e.g., **NBP-COOH** versus **NBP-H** by $SO_4^{-•}$; C_nF_{2n+1}−CH_2CH_2−COO^- versus HC_2F_{2n}−COO^- by $HO^•$[18]). In addition, if the original unknown PFAS molecule does not contain a C−H bond or −COO^-, it would escape from target analysis. For these reasons, the TOP assay is less accurate than combustion ion chromatography[34] for total F quantitation, but it can be very informative for qualitative analysis and may play a critical role in identifying original PFAS structures.

Second, experimental results have shown that a majority of PFAS structures cannot be fully mineralized by either $SO_4^{-•}$ or $HO^•$. If a large excess of $SO_4^{-•}$ could deplete key −COO^--containing products, using different oxidant doses may alter the product presence or dominance (Figure 2a). This feature is unique to $SO_4^{-•}$ oxidation. For comparison, the oxidation of **NBP-H**, **6:3 FTCA**, and **6:2 FTSA** with $HO^•$ resulted in rather consistent product spectra regardless of the oxidant dose (Figure 2b). It is also noteworthy that $SO_4^{-•}$ or $HO^•$ can have very different product dominance for the legacy fluorotelomers (Figure 2c). The complementary use of both radicals will lead to novel information toward deducing the structures of the original "PFAS precursors". Other oxidation methods, such as cobalt-activated peroxymonosulfate at 20 °C are also worth exploring. In a recent report, the oxidation of **6:2 FTSA** (40 μM) using 5 mM of $KHSO_5$ and 50 μM $CoSO_4$ yielded n = 5 PFHxA as the dominant TP.[35]

We highlight the importance of exploring the transformation mechanisms and pathways for oxidizable PFAS molecules. The detection of TFA as the only PFCA product from Nafion-related PFESAs is a novel example. The H−CF($\mathbf{CF_3}$)−O− or $^-$OOC−CF($\mathbf{CF_3}$)−O− are oxidized and then transformed into $\mathbf{CF_3}$−C(O)−O− (Scheme 1), which further hydrolyzes to yield TFA. **TP2** is another novel indicator for PFESAs with a −O−CF_2CF_2−SO_3^- terminal, a common structure shared in Nafion-related (Figure 1), F-53B, and other novel structural analogues.[5,6,36] Previous studies also identified other PFAS transformation patterns under $HO^•$ oxidation, such as the exclusive formation of C_7F_{15}−COO^- from C_8F_{17}−SO_2NH_2[15] and the dominating formation of $^-$OOC−$C_{n-1}F_{2n-2}$−COO^- from H−CF_2−$C_{n-1}F_{2n-2}$−COO^- (Figure 2d).[18] We recommend (i) pretreating the samples with both $HO^•$ and $SO_4^{-•}$ (and sequential treatment, if needed) before target PFAS analysis, (ii) adding more known structures (e.g., $^-$OOC−C_nF_{2n}−COO^-, ether carboxylates/sulfonates, and other commercially available PFAS chemicals) to the target list of TOP assay, (iii) using advanced mass spectrometry methodologies,[37] data processing algorithms,[38] and additional spectroscopy methods (e.g., ^{19}F NMR) to assist structural determination, and (iv) modifying the existing methodologies with new structural transformation mechanisms. In order to satisfy the imminent need for the detection, monitoring, and treatment of "non-legacy" PFAS pollutants, it is imperative to expand our understanding of structure-transformation relationships for emerging PFAS chemicals.[18−20,36] The elucidation of additional

https://doi.org/10.1021/acs.est.3c06289
Environ. Sci. Technol. 2024, 58, 6415−6424

transformation pathways for $SO_4^{-\bullet}$ oxidation is equally important and intriguing to environmental chemists. The currently unknown $SO_4^{-\bullet}$ oxidation TPs might soon become the "signature" of certain PFAS pollutants.

Lastly, PFAS analytical works have not adopted the widely used acidic persulfate digestion for environmental samples. We expect this report to trigger interest in testing $SO_4^{-\bullet}$ oxidation (simply adjust the $S_2O_8^{2-}$ solution pH to 2.0 and run a few additional LC−MS samples) in specific PFAS analytical scenarios[14] to obtain more critical information on pollutant structures and profiles.

Validation with an "Environmentally Relevant" Demonstration. Here we validate the aforementioned trends of TP formation and the recommended strategies for probing PFAS precursors using acidic persulfate digestion. We set the scenario as analyzing a water sample contaminated by both legacy (from fire-fighting activities) and emerging PFAS (from fluoropolymer manufacturing) with a triple quadrupole mass spectrometer (LC−MS/MS) for quantifying target PFAS at low concentrations. An aqueous film-forming foam (AFFF, containing ∼10 g L^{-1} of organic fluorine[34] and ∼950 g L^{-1} of organic carbon) was diluted by 100000-fold and then spiked with 0.35 μM of **NBP-COOH**. ^{19}F NMR characterization (Figure S1) and degradation experiments of the AFFF have confirmed its dominant PFAS species as a C_6F_{13}−fluorotelomer structure.[39] Hence, the resulting solution contained 93 μg L^{-1} of F from **NBP-COOH**, ∼100 μg L^{-1} of F from fluorotelomer-based surfactants, and 9.5 mg L^{-1} of organic carbon. After oxidation by 5, 20, and 60 mM $K_2S_2O_8$ at acidic and alkaline pH, the analyses by a third-party LC−MS/MS (Table 5) showed consistent results with our earlier findings from using 0.5 mM individual PFAS and 5−100 mM $K_2S_2O_8$ without an organic matrix.

Because the current TOP assay protocol involved only alkaline persulfate digestion, the detection of a PFCA mixture (Table 5, zone K) was not sufficient to interpret the precursor structure. If one applies the "n − 2 dominance" rule,[15,17] the dominance of PFPeA (C_4F_9−COO^-) and relatively constant abundance of other PFCA products (regardless of the persulfate dose) could be attributed to a C_6F_{13}−CH_2CH_2−X fluorotelomer. However, it is also possible that each PFCA was individually derived from the corresponding sulfonamide (Figure 2d)[15] used in early AFFF products.[40−42] At this point, acidic persulfate digestion provided additional clues (Table 5, zone L). When the persulfate dose was low, the "n − 1" PFHxA (C_5F_{11}−COO^-) was the dominant product. As the persulfate dose increased, the product dominance shifted to shorter-chain PFCAs. This trend is consistent with our earlier results (Figure 2a for **6:3 FTCA** at various persulfate doses; Figure 2c for various ***n*:3 FTCAs** at a low persulfate dose). Therefore, one could be more confident in assigning the primary precursor as a C_6F_{13}−CH_2CH_2−X fluorotelomer. Notably, when the AFFF was diluted 10000× (thus containing 95 mg L^{-1} of organic carbon and consuming more oxidants), the similar PFCA product profiles were observed (Table 5, zone M).

Regarding the detection of Nafion-related PFAS, **TP2** (^-OOC−CF_2−SO_3^-) was not found in the samples after alkaline persulfate digestion (Table 5, zone K). The low concentration of **TP1** could be attributed to a small chance of **NBP-COOH** oxidation by $SO_4^{-\bullet}$ (before reacting with HO^-, also see Table 1, entry 2). In contrast, acid persulfate digestion generated significant yields of **TP1** and **TP2** (Table 5, zones L and M). Furthermore, **TP2** was not produced from the acid persulfate digestion of AFFF (Table 5, zone N versus M). Therefore, if the simple chemical **TP2** is used as an analytical standard, its detection after acid persulfate digestion could indicate some novel PFAS beyond the legacy AFFF-relevant structures. For comparison, the current TOP assay protocol using alkaline persulfate digestion and conventional PFCA analytical standards would not catch Nafion-related PFAS.

Therefore, acidic persulfate digestion for the TOP assay allows the transformation of perfluorinated carboxylates into simpler PFAS structures for target analysis. Its combination with alkaline persulfate digestion will enhance flexibility and confidence in discovering and tracking emerging PFAS pollutants. Like the original TOP assay reported in 2012,[15] this "new" approach warrants further evaluation, development, and optimization for various scenarios and needs.

■ ASSOCIATED CONTENT

Supporting Information

The Supporting Information is available free of charge at https://pubs.acs.org/doi/10.1021/acs.est.3c06289.

Information on PFAS chemicals and alkaline hydrolysis of acyl fluoride and sulfonyl fluoride structures, details of instrument settings and QA/QC of HPLC−HRMS analyses, and additional data on defluorination of all PFAS structures by both $SO_4^{-\bullet}$ and $HO^\bullet$ (PDF)

■ AUTHOR INFORMATION

Corresponding Author

Jinyong Liu − *Department of Chemical & Environmental Engineering, University of California, Riverside, California 92521, United States;* orcid.org/0000-0003-1473-5377; Email: jinyongl@ucr.edu, jinyong.liu101@gmail.com

Authors

Zekun Liu − *Department of Chemical & Environmental Engineering, University of California, Riverside, California 92521, United States; Claros Technologies Inc., Minneapolis, Minnesota 55413, United States;* orcid.org/0000-0003-3802-2662

Bosen Jin − *Department of Chemical & Environmental Engineering, University of California, Riverside, California 92521, United States;* orcid.org/0000-0001-7659-3437

Dandan Rao − *Department of Chemical & Environmental Engineering, University of California, Riverside, California 92521, United States*

Michael J. Bentel − *Department of Chemical & Environmental Engineering, University of California, Riverside, California 92521, United States;* orcid.org/0000-0003-1404-113X

Tianchi Liu − *Department of Chemical & Environmental Engineering, University of California, Riverside, California 92521, United States*

Jinyu Gao − *Department of Chemical & Environmental Engineering, University of California, Riverside, California 92521, United States;* orcid.org/0000-0002-1751-3430

Yujie Men − *Department of Chemical & Environmental Engineering, University of California, Riverside, California 92521, United States;* orcid.org/0000-0001-9811-3828

Complete contact information is available at: https://pubs.acs.org/10.1021/acs.est.3c06289

Author Contributions

Z.L. conducted most experiments, analyzed the data, and drafted the manuscript; B.J. and Y.M. assisted in HPLC−HRMS

https://doi.org/10.1021/acs.est.3c06289
Environ. Sci. Technol. 2024, 58, 6415−6424

measurements; D.R. conducted tests of the diluted AFFF + NBP-COOH solution mixtures; M.J.B. characterized the AFFF in earlier studies; T.L. assisted in ^{19}F NMR characterization of NBP structures; J.G. contributed additional data on oxidative conversion; J.L. conceived the idea, supervised the research, and revised the manuscript.

Notes

The authors declare no competing financial interest.

■ ACKNOWLEDGMENTS

Financial support was provided by the Strategic Environmental Research and Development Program (WP21-1071 and ER22-3184 for Z.L. and J.L.; ER20-1541 for B.J. and Y.M.). Drs. Zijie Xia, John Brockgreitens, Terrance P. Smith, and Michelle Bellanca at the PFAS Analytical Lab of Claros Technologies Inc. supported the LC−MS/MS analyses in the section of method validation with diluted AFFF + NBP-COOH.

■ REFERENCES

(1) Evich, M. G.; Davis, M. J.; McCord, J. P.; Acrey, B.; Awkerman, J. A.; Knappe, D. R.; Lindstrom, A. B.; Speth, T. F.; Tebes-Stevens, C.; Strynar, M. J.; et al. Per-and polyfluoroalkyl substances in the environment. *Science* **2022**, *375*, No. eabg9065.

(2) Kwiatkowski, C. F.; Andrews, D. Q.; Birnbaum, L. S.; Bruton, T. A.; DeWitt, J. C.; Knappe, D. R.; Maffini, M. V.; Miller, M. F.; Pelch, K. E.; Reade, A.; et al. Scientific basis for managing PFAS as a chemical class. *Environ. Sci. Technol. Lett.* **2020**, *7*, 532−543.

(3) Lohmann, R.; Cousins, I. T.; DeWitt, J. C.; Gluge, J.; Goldenman, G.; Herzke, D.; Lindstrom, A. B.; Miller, M. F.; Ng, C. A.; Patton, S.; et al. Are fluoropolymers really of low concern for human and environmental health and separate from other PFAS? *Environ. Sci. Technol.* **2020**, *54*, 12820−12828.

(4) Strynar, M.; Dagnino, S.; McMahen, R.; Liang, S.; Lindstrom, A.; Andersen, E.; McMillan, L.; Thurman, M.; Ferrer, I.; Ball, C. Identification of novel perfluoroalkyl ether carboxylic acids (PFECAs) and sulfonic acids (PFESAs) in natural waters using accurate mass time-of-flight mass spectrometry (TOFMS). *Environ. Sci. Technol.* **2015**, *49*, 11622−11630.

(5) McCord, J.; Strynar, M. Identification of per-and polyfluoroalkyl substances in the Cape Fear River by high resolution mass spectrometry and nontargeted screening. *Environ. Sci. Technol.* **2019**, *53*, 4717−4727.

(6) Wang, S.; Huang, J.; Yang, Y.; Hui, Y.; Ge, Y.; Larssen, T.; Yu, G.; Deng, S.; Wang, B.; Harman, C. First report of a Chinese PFOS alternative overlooked for 30 years: Its toxicity, persistence, and presence in the environment. *Environ. Sci. Technol.* **2013**, *47*, 10163−10170.

(7) Washington, J. W.; Rosal, C. G.; McCord, J. P.; Strynar, M. J.; Lindstrom, A. B.; Bergman, E. L.; Goodrow, S. M.; Tadesse, H. K.; Pilant, A. N.; Washington, B. J.; et al. Nontargeted mass-spectral detection of chloroperfluoropolyether carboxylates in New Jersey soils. *Science* **2020**, *368*, 1103−1107.

(8) Guillette, T. C.; McCord, J.; Guillette, M.; Polera, M. E.; Rachels, K. T.; Morgeson, C.; Kotlarz, N.; Knappe, D. R. U.; Reading, B. J.; Strynar, M.; Belcher, S. M. Elevated levels of per- and polyfluoroalkyl substances in Cape Fear River striped bass (*Morone saxatilis*) are associated with biomarkers of altered immune and liver function. *Environ. Int.* **2020**, *136*, No. 105358.

(9) Conley, J. M.; Lambright, C. S.; Evans, N.; Medlock-Kakaley, E.; Hill, D.; McCord, J.; Strynar, M. J.; Wehmas, L. C.; Hester, S.; MacMillan, D. K.; et al. Developmental toxicity of Nafion byproduct 2 (NBP2) in the Sprague-Dawley rat with comparisons to hexafluoropropylene oxide-dimer acid (HFPO-DA or GenX) and perfluorooctane sulfonate (PFOS). *Environ. Int.* **2022**, *160*, No. 107056.

(10) Gui, W.; Guo, H.; Wang, J.; Wang, C.; Guo, Y.; Zhang, K.; Dai, J.; Zhao, Y. Nafion by-product 2 disturbs lipid homeostasis in zebrafish embryo. *Environ. Pollut.* **2023**, *322*, No. 121178.

(11) Gui, W.; Guo, H.; Chen, X.; Wang, J.; Guo, Y.; Zhang, H.; Zhou, X.; Zhao, Y.; Dai, J. Emerging polyfluorinated compound Nafion by-product 2 disturbs intestinal homeostasis in zebrafish (Danio rerio). *Ecotoxicology and Environmental Safety* **2023**, *249*, No. 114368.

(12) He, Y.; Lv, D.; Li, C.; Liu, X.; Liu, W.; Han, W. Human exposure to F-53B in China and the evaluation of its potential toxicity: An overview. *Environ. Int.* **2022**, *161*, No. 107108.

(13) Mahoney, H.; Xie, Y.; Brinkmann, M.; Giesy, J. P. Next generation per- and poly-fluoroalkyl substances: Status and trends, aquatic toxicity, and risk assessment. *Eco-Environment & Health* **2022**, *1*, 117−131.

(14) Ateia, M.; Chiang, D.; Cashman, M.; Acheson, C. Total oxidizable precursor (TOP) assay—Best practices, capabilities and limitations for PFAS site investigation and remediation. *Environ. Sci. Technol. Lett.* **2023**, *10*, 292−301.

(15) Houtz, E. F.; Sedlak, D. L. Oxidative conversion as a means of detecting precursors to perfluoroalkyl acids in urban runoff. *Environ. Sci. Technol.* **2012**, *46*, 9342−9349.

(16) Martin, D.; Munoz, G.; Mejia-Avendaño, S.; Duy, S. V.; Yao, Y.; Volchek, K.; Brown, C. E.; Liu, J.; Sauvé, S. Zwitterionic, cationic, and anionic perfluoroalkyl and polyfluoroalkyl substances integrated into total oxidizable precursor assay of contaminated groundwater. *Talanta* **2019**, *195*, 533−542.

(17) Liu, Z.; Bentel, M. J.; Yu, Y.; Ren, C.; Gao, J.; Pulikkal, V. F.; Sun, M.; Men, Y.; Liu, J. Near-quantitative defluorination of perfluorinated and fluorotelomer carboxylates and sulfonates with integrated oxidation and reduction. *Environ. Sci. Technol.* **2021**, *55*, 7052−7062.

(18) Gao, J.; Liu, Z.; Bentel, M. J.; Yu, Y.; Men, Y.; Liu, J. Defluorination of omega-hydroperfluorocarboxylates (ω-HPFCAs): Distinct reactivities from perfluoro and fluorotelomeric carboxylates. *Environ. Sci. Technol.* **2021**, *55*, 14146−14155.

(19) Zhang, C.; Hopkins, Z. R.; McCord, J.; Strynar, M. J.; Knappe, D. R. Fate of per-and polyfluoroalkyl ether acids in the total oxidizable precursor assay and implications for the analysis of impacted water. *Environ. Sci. Technol. Lett.* **2019**, *6*, 662−668.

(20) Zhang, C.; Tang, T.; Knappe, D. R. U. Oxidation of per- and polyfluoroalkyl ether acids and other per- and polyfluoroalkyl substances by sulfate and hydroxyl radicals: Kinetic insights from experiments and models. *Environ. Sci. Technol.* **2023**, *57*, 18970−18980.

(21) Menzel, D. W.; Corwin, N. The measurement of total phosphorus in seawater based on the liberation of organically bound fractions by persulfate oxidation 1. *Limnology and Oceanography* **1965**, *10*, 280−282.

(22) Liu, J.; Wang, H.; Yang, H.; Ma, Y.; Cai, O. Detection of phosphorus species in sediments of artificial landscape lakes in China by fractionation and phosphorus-31 nuclear magnetic resonance spectroscopy. *Environ. Pollut.* **2009**, *157*, 49−56.

(23) Hori, H.; Yamamoto, A.; Hayakawa, E.; Taniyasu, S.; Yamashita, N.; Kutsuna, S.; Kiatagawa, H.; Arakawa, R. Efficient decomposition of environmentally persistent perfluorocarboxylic acids by use of persulfate as a photochemical oxidant. *Environ. Sci. Technol.* **2005**, *39*, 2383−2388.

(24) Zhang, Y.; Moores, A.; Liu, J.; Ghoshal, S. New insights into the degradation mechanism of perfluorooctanoic acid by persulfate from density functional theory and experimental data. *Environ. Sci. Technol.* **2019**, *53*, 8672−8681.

(25) Marchione, A. A.; Diaz, E. L.; Boyle, J. E. Kinetics of aqueous persulfate-induced oxidative degradation of heptafluorobutanoate, pentafluoropropionate, and trifluoroacetate. *J. Fluorine Chem.* **2021**, *252*, No. 109902.

(26) Ding, X.; Song, X.; Chen, X.; Ding, D.; Xu, C.; Chen, H. Degradation and mechanism of hexafluoropropylene oxide dimer acid by thermally activated persulfate in aqueous solutions. *Chemosphere* **2022**, *286*, No. 131720.

(27) Seko, M. The ion-exchange membrane, chlor-alkali process. *Industrial & Engineering Chemistry Product Research and Development* **1976**, *15*, 286−292.

https://doi.org/10.1021/acs.est.3c06289
Environ. Sci. Technol. 2024, 58, 6415−6424

(28) Bébin, P.; Caravanier, M.; Galiano, H. Nafion®/clay-SO_3H membrane for proton exchange membrane fuel cell application. *J. Membr. Sci.* **2006**, *278*, 35−42.
(29) Robuck, A. R.; Cantwell, M. G.; McCord, J. P.; Addison, L. M.; Pfohl, M.; Strynar, M. J.; McKinney, R.; Katz, D. R.; Wiley, D. N.; Lohmann, R. Legacy and novel per- and polyfluoroalkyl substances in juvenile seabirds from the U.S. Atlantic coast. *Environ. Sci. Technol.* **2020**, *54*, 12938−12948.
(30) Robuck, A. R.; McCord, J. P.; Strynar, M. J.; Cantwell, M. G.; Wiley, D. N.; Lohmann, R. Tissue-specific distribution of legacy and novel per- and polyfluoroalkyl substances in juvenile seabirds. *Environ. Sci. Technol. Lett.* **2021**, *8*, 457−462.
(31) Yao, J.; Pan, Y.; Sheng, N.; Su, Z.; Guo, Y.; Wang, J.; Dai, J. Novel perfluoroalkyl ether carboxylic acids (PFECAs) and sulfonic acids (PFESAs): Occurrence and association with serum biochemical parameters in residents living near a fluorochemical plant in China. *Environ. Sci. Technol.* **2020**, *54*, 13389−13398.
(32) Stefanidis, D.; Jencks, W. P. General base catalysis of ester hydrolysis. *J. Am. Chem. Soc.* **1993**, *115*, 6045−6050.
(33) Yates, K.; McClelland, R. A. Mechanisms of ester hydrolysis in aqueous sulfuric acids. *J. Am. Chem. Soc.* **1967**, *89*, 2686−2692.
(34) Han, Y.; Pulikkal, V. F.; Sun, M. Comprehensive validation of the adsorbable organic fluorine analysis and performance comparison of current methods for total per-and polyfluoroalkyl substances in water samples. *ACS ES&T Water* **2021**, *1*, 1474−1482.
(35) Zhang, Y.; Liu, J.; Moores, A.; Ghoshal, S. Transformation of 6:2 fluorotelomer sulfonate by cobalt (II)-activated peroxymonosulfate. *Environ. Sci. Technol.* **2020**, *54*, 4631−4640.
(36) Gao, J.; Liu, Z.; Chen, Z.; Rao, D.; Che, S.; Gu, C.; Men, Y.; Huang, J.; Liu, J. Photochemical degradation pathways and near-complete defluorination of chlorinated polyfluoroalkyl substances. *Nature Water* **2023**, *1*, 381−390.
(37) Zweigle, J.; Bugsel, B.; Röhler, K.; Haluska, A. A.; Zwiener, C. PFAS-contaminated soil site in Germany: Nontarget screening before and after direct TOP assay by Kendrick mass defect and FindPFΔS. *Environ. Sci. Technol.* **2023**, *57*, 6647−6655.
(38) Antell, E. H.; Yi, S.; Olivares, C. I.; Ruyle, B. J.; Kim, J. T.; Tsou, K.; Dixit, F.; Alvarez-Cohen, L.; Sedlak, D. L. The total oxidizable precursor (TOP) assay as a forensic tool for per- and polyfluoroalkyl substances (PFAS) source apportionment. *ACS ES&T Water* **2024**, *4*, 948−957.
(39) Liu, J.; Lin, S.; Sun, M. Final Report: ER18-1497 High-Performance Treatment of PFAS from Investigation-Derived Waste: Integrating Advanced Oxidation-Reduction and Membrane Concentration. *SERDP*, 2020.
(40) Place, B. J.; Field, J. A. Identification of novel fluorochemicals in aqueous film-forming foams used by the US military. *Environ. Sci. Technol.* **2012**, *46*, 7120−7127.
(41) Houtz, E. F.; Higgins, C. P.; Field, J. A.; Sedlak, D. L. Persistence of perfluoroalkyl acid precursors in AFFF-impacted groundwater and soil. *Environ. Sci. Technol.* **2013**, *47*, 8187−8195.
(42) Nickerson, A.; Rodowa, A. E.; Adamson, D. T.; Field, J. A.; Kulkarni, P. R.; Kornuc, J. J.; Higgins, C. P. Spatial trends of anionic, zwitterionic, and cationic PFASs at an AFFF-impacted site. *Environ. Sci. Technol.* **2021**, *55*, 313−323.

https://doi.org/10.1021/acs.est.3c06289
Environ. Sci. Technol. 2024, 58, 6415−6424